Unidirectional rotary nanomotors powered by an electrochemical potential gradient

A. Yu. Smirnov[1,2], S. Savel'ev[1,3], L. G. Mourokh[1,4], and Franco Nori[1,5]

Frontier Research System, The Institute of Physical and Chemical Research (RIKEN), Wako-shi, Saitama, 351-0198, Japan

[2] *CREST, Japan Science and Technology Agency, Kawaguchi, Saitama, 332-0012, Japan*

[3] *Department of Physics, Loughborough University, Loughborough LE11 3TU, UK*

[4] *Department of Engineering Science and Physics, College of Staten Island, The City University of New York, Staten Island, New York 10314, USA*

[5] *Center for Theoretical Physics, Physics Department, The University of Michigan, Ann Arbor, MI 48109-1040, USA*

(Dated: February 2, 2008)

Abstract

We examine the dynamics of biological nanomotors within a simple model of a rotor having three ion-binding sites. It is shown that in the presence of an external dc electric field in the plane of the rotor, the loading of the ion from the positive side of a membrane (rotor charging) provides a torque leading to the motor rotation. We derive equations for the proton populations of the sites and solve these equations numerically jointly with the Langevin-type equation for the rotor angle. Using parameters for biological systems, we demonstrate that the sequential loading and unloading of the sites lead to the unidirectional rotation of the motor. The previously unexplained phenomenon of fast direction-switching in the rotation of a bacterial flagellar motor can also be understood within our model.

PACS numbers: 87.16.Ac, 85.85.+j

Biological rotary motors provide remarkable examples of how electrochemical energy can be efficiently converted into mechanical motion [1, 2]. Two of the most important representatives of this family, the F_0 motor of ATP (adenosine triphosphate) synthase (F_1F_0–ATPase) and the bacterial flagellar motor (BFM), are powered by H^+ or Na^+ ions, which flow down the electrochemical gradient across the mitochondrial or cell membranes, thereby generating a torque [3, 4]. Hereafter we concentrate on proton-driven motors, but the same considerations are valid for sodium-driven motors as well. The gradient of the electrochemical potential is maintained by the metabolic mechanism translocating protons from the negative side of the membrane to its positive side [1, 5].

Both of these rotary motors have similar components: (i) a stator, tightly attached to the membrane, and (ii) a ring-shaped rotor, which can freely rotate around its axis. The rotor part of the F_0 motor is mechanically coupled to the F_1 domain of ATP synthase, whereas the rotor of the BFM is linked to the propeller. It is assumed [3] that the rotor has several (10 to 14) proton-binding sites. The permanent generation of the torque can be derived from the electrostatic interaction between stator charges and charges of the rotor sites which bias the thermal diffusion of the rotor in a specific direction [3, 6]. This Brownian ratchet mechanism can generate a torque of about 40 pN·nm corresponding to a realistic rate of ATP synthesis [3]. However, both the power stroke and Brownian ratchet models, exploiting "constructive" features of Brownian motion, do not succeed in explaining the amazing performance of the bacterial flagellar motor, generating a torque of 2700 - 4600 pN·nm with an efficiency of about 90% [4]. The ability of the BFM to rapidly switch the direction of the rotation remains unexplained as well, because transport in ratchets (see, e.g., the reviews in [7]) is usually fully controlled by a *fixed* asymmetry of the potential energy. These facts point to the possibility that the BFM can use the energy stored in the proton electrochemical gradient *directly*, without a mediation of the Brownian motion [6].

Here we explore a simple model mimicking important features of real biomolecular rotary motors and allowing a quantitative treatment based on methods of condensed matter physics [8]. These approaches have been previously applied to nanoelectromechanical systems (NEMS) with their mechanical motion affecting the electrical properties of electronic devices [9]. Similar processes take place in nanoscale biological objects, where electrical and mechanical degrees of freedom are also strongly coupled, making them living counterparts to artificial NEMS. Note that only nano-oscillators have been extensively studied by

theorists, although a single-molecule rotor and a nanoelectromechanical rotational actuator [10] have been demonstrated experimentally. To the best of our knowledge, no theoretical investigations of rotary NEMS have been reported yet.

Model. The system under consideration here consists of *three* equally-spaced proton-binding sites A, B, C attached to the rotating ring (rotor) in the presence of a constant y-directed electric force $\mathbf{F}$ (see the inset in Fig.1). The rotor sites can be coupled to two proton sources S_1 and S_2 as well as to the proton drain D, connected to the proton reservoir with a low electrochemical potential μ_D (the negative side of the membrane). The source leads S_1 and S_2 can be connected (or disconnected) at will to the proton reservoir with a higher electrochemical potential μ_S (the positive or P-side of the membrane). We show below that the activation of the lead S_1 results in a clockwise motion of the rotor, whereas connecting the S_2-lead to the P-side of the membrane (and disconnecting the S_1-lead) generates a counterclockwise rotation. At each instant of time only one source lead is coupled to the P-side proton reservoir.

The Hamiltonian of the system has the form:

$$H = \frac{p^2}{2Mr_0^2} - U_0 \sum_{\sigma} n_\sigma \cos(\phi + \phi_\sigma) + \sum_{\sigma} E_\sigma n_\sigma + \sum_{k\alpha} E_{k\alpha} c^+_{k\alpha} c_{k\alpha} + \sum_{\sigma\sigma'} U_{\sigma\sigma'} n_\sigma n_{\sigma'} + H_{\rm tun} + H_Q, \quad (1)$$

where ϕ is the angle of rotation, $p = -i\hbar(\partial/\partial\phi)$ is the operator of angular momentum of the rotator with radius r_0 and effective mass M. We take into account here the effects of a constant y-directed external electric field, with a potential energy profile $U(\phi) = -U_0 \cos\phi$, on the protons localized in the three sites $\sigma = A, B, C$ with positions, characterized by the angles ϕ_A, ϕ_B, ϕ_C, respectively. The operators a^+_σ, a_σ describe the creation and annihilation of a proton on the site (dot) σ with a population $n_\sigma = a^+_\sigma a_\sigma$, whereas the operators $c^+_{k\alpha}, c_{k\alpha}$ are related to the k-state of the proton in the source and drain reservoirs (leads) with energy $E_{k\alpha}$ ($\alpha = S_1, S_2, D$). The Coulomb repulsion between protons is given by the potentials $U_{\sigma\sigma'}$. The tunneling coupling between dots and leads is given by the Hamiltonian

$$H_{\rm tun} = -\sum_{k\alpha\sigma} T_{k\alpha} c^+_{k\alpha} a_\sigma w_{\alpha\sigma}(\phi) + h.c.,$$

where the tunneling amplitudes $T_{k\alpha}$ are multiplied by the factor

$$w_{\alpha\sigma}(\phi) = \exp\left[-\frac{\sqrt{2} r_0}{\lambda} \sqrt{1 - \cos(\phi + \phi_\sigma - \phi_\alpha)} \right],$$

which reflects an exponential dependence of the tunneling rate on the distance between the $\sigma-$dot and the $\alpha-$lead with a characteristic spatial scale λ. To take into account the influence of the classical dissipative environment $\{Q\}$ with the Hamiltonian $H_{\rm Bath}$ on the rotational degrees of freedom, we include the term $H_Q = -r_0\,\phi\,Q + H_{\rm Bath}$ in Eq.(1). Here Q is the bath variable, which can be represented as a sum of the fluctuating part, $Q^{(0)}$, and the bath response on the action of the rotator, $Q = Q^{(0)} - \zeta r_0\dot{\phi}$, where the coupling of the rotor to the bath is characterized by the drag coefficient ζ. The unperturbed bath variables $Q^{(0)}$ have Gaussian statistics with zero average, $\langle Q^{(0)}\rangle = 0$, and the correlation function, $\langle Q^{(0)}(t)Q^{(0)}(t')\rangle = 2\zeta T\delta(t-t')$, where T is the temperature of the environment ($k_B = 1$). The Brownian motion of the nanorotator is governed by the Langevin equation

$$\ddot{\phi} + \gamma\dot{\phi} + \frac{U_0}{Mr_0^2}\sum_\sigma n_\sigma \sin(\phi+\phi_\sigma) = \xi, \tag{2}$$

where γ is the damping rate of the rotator, $\gamma = \zeta/M$, and the Gaussian fluctuation source $\xi = Q^{(0)}/(Mr_0)$ is characterized by the correlation function: $\langle\xi(t)\xi(t')\rangle = 2\gamma(T/Mr_0^2)\delta(t-t')$. The influence of the proton tunneling events, $\sim -\partial H_{\rm tun}/\partial\phi$, on the mechanical motion is assumed to be negligibly small here.

To describe the process of loading and unloading of proton-binding sites A, B, and C, we introduce the proton vacuum state $|1\rangle = |{\rm Vac}\rangle$, jointly with seven additional states, $|2\rangle = a_A^+|1\rangle,\ |3\rangle = a_B^+|1\rangle,\ |4\rangle = a_A^+a_B^+|1\rangle,\ |5\rangle = a_C^+|1\rangle, |6\rangle = a_A^+a_C^+|1\rangle,\ |7\rangle = a_B^+a_C^+|1\rangle,\ |8\rangle = a_A^+a_B^+a_C^+|1\rangle$. Each of the proton operators can be expressed in terms of operators $\rho_{\mu\nu} = |\mu\rangle\langle\nu|$ $(\mu,\nu = 1,..,8)$. In particular, the operator a_σ has the form: $a_\sigma = \sum_{\mu\nu} a_{\sigma;\mu\nu}\rho_{\mu\nu}$, with the following non-zero matrix elements: $a_{A;12} = a_{A;34} = a_{A;56} = a_{A;78} = 1; a_{B;13} = -a_{B;24} = a_{B;57} = -a_{B;68} = 1; a_{C;15} = -a_{C;26} = -a_{C;37} = a_{C;48} = 1$. The populations of the dots, $n_\sigma = a_\sigma^+a_\sigma$, are expressed in terms of the diagonal operators $\rho_\mu \equiv \rho_{\mu\mu}$, as: $n_A = \rho_2+\rho_4+\rho_6+\rho_8,\ n_B = \rho_3+\rho_4+\rho_7+\rho_8,\ n_C = \rho_5+\rho_6+\rho_7+\rho_8$. Thus, for the protons localized on the rotor sites A, B, C we obtain the Hamiltonian $H_{ABC} = \sum_{\mu=1}^8 \epsilon_\mu|\mu\rangle\langle\mu|$, with an energy spectrum depending on the local value of the rotor angle ϕ: $\epsilon_1 = 0,\ \epsilon_2 = E_A - U_0\cos(\phi+\phi_A),\ \epsilon_3 = E_B - U_0\cos(\phi+\phi_B),\ \epsilon_4 = \epsilon_2+\epsilon_3,\ \epsilon_5 = E_C - U_0\cos(\phi+\phi_C),\ \epsilon_6 = \epsilon_2+\epsilon_5,\ \epsilon_7 = \epsilon_3+\epsilon_5,\ \epsilon_8 = \epsilon_2+\epsilon_3+\epsilon_5$. We assume here that the characteristic time of proton tunneling to and out of the proton-binding sites, γ^{-1}, is much shorter than the the time scale of the rotary angle, $\langle\dot{\phi}\rangle^{-1}$, and that the noise produced by the proton tunneling between the sites and the source and drain contacts has much less effect on the mechanical motion of the

rotor than the noise ξ generated by the bath $\{Q\}$. Accordingly, we can average the stochastic Eq.(2) over fluctuations of the proton reservoirs without averaging over the fluctuations of the mechanical heat bath. The partially averaged proton population n_σ involved in Eq.(2) depends on the local fluctuating value of the rotational angle ϕ. To determine these populations, we derive the following master equation for the proton distribution ρ_μ, averaged over reservoirs fluctuations,

$$\dot{\rho}_\mu + \gamma_\mu \rho_\mu = \sum_\nu \gamma_{\mu\nu}\rho_\nu, \quad \text{with} \tag{3}$$

$$\gamma_{\mu\nu} = \sum_{\alpha\sigma} \Gamma_\alpha(\phi)\{|a_{\sigma;\mu\nu}|^2[1 - f_\alpha(\omega_{\nu\mu})] + |a_{\sigma;\nu\mu}|^2 f_\alpha(\omega_{\mu\nu})\},$$

$\gamma_\mu = \sum_\nu \gamma_{\nu\mu}$, and $\Gamma_\alpha(\phi) = \Gamma_\alpha |w_{\alpha\sigma}(\phi)|^2$. Also: $\omega_{\mu\nu} = \epsilon_\mu - \epsilon_\nu$ ($\hbar = 1$), $\Gamma_\alpha = 2\pi \sum_k |T_{k\alpha}|^2 \delta(\omega - \omega_{\mu\nu})$ [8]. The protons in the reservoirs are characterized by the Fermi distributions, $f_\alpha(\omega) = \left[\exp(\frac{\omega-\mu_\alpha}{T}) + 1\right]^{-1}$, with temperature T and electrochemical potentials $\mu_S = V/2, \mu_D = -V/2$, where V is the proton voltage build-up. We include the absolute value of the proton charge, $|e|$, into the definition of the voltage V and measure the voltage in units of energy, meV. Notice that, despite of the averaging over proton reservoirs, the master equation, Eq.(3), contains a stochastic component, which is determined by the fluctuations of the rotor angle $\phi(t)$, taken at the same time t. Eq.(3) is valid for weak coupling between dots and leads, and for the case when the angular coordinate $\phi(t)$ does not change significantly on the characteristic time scale, $\tau_T = \pi/T$, of the Fermi distribution.

We consider here the rotation of the system with the parameters roughly corresponding to the rotor part of the bacterial flagellar motor [11], which has mass $M = 5000$ kDa $= 8.3 \times 10^{-21}$ kg and a radius $r_0 = 15$ nm. Three torque-generating sites, A, B, and C, are attached at the points $\phi_A = 0$, $\phi_B = 2\pi/3$, and $\phi_C = -2\pi/3$, respectively. The locations of the two possible source contacts S_1, S_2 and the drain D are defined as $\phi_{S_1} = -2\pi/3$, $\phi_{S_2} = 2\pi/3$, $\phi_D = 0$. For the Coulomb interaction between sites located a distance $r_0\sqrt{3}$ apart, in a medium with a dielectric constant $\varepsilon_r \sim 4$, we obtain: $U_{ab} \simeq U_{bc} \simeq U_{ac} \simeq 15$ meV. We choose an intermediate value of the drag coefficient $\zeta = 30$ pN s/m, which is related to the motion of a sphere with radius $r_0 = 15$ nm in an environment with a viscosity of 0.1 mPa·s. The rotational damping rate is quite high, $\gamma = 3.6$ ns^{-1}, which means that the free rotations of the motor come to an end after a time interval of the order $\gamma^{-1} \sim 300$ ps.

Results. In Fig.1a we present a schematic diagram of the rotor ring, jointly with the time

dependence of the number of full rotations $\phi(t)/2\pi$, obtained from the numerical solution of the Langevin equation, Eq.(2), and the master equations, Eqs.(3), at the source-drain voltage $V = \mu_S - \mu_D = 500$ meV, the external potential $U_0 = 200$ meV, the tunneling couplings to the leads $\Gamma_L = \Gamma_R = 10^9$ s^{-1}, and at temperature $T = 300$ K. The source contact S_1 is activated, and, accordingly, the rotor moves in the clockwise (positive) direction and performs more than four full rotations in $\sim$10 μs. We start here with a slightly shifted initial position of the rotor, when $\phi(0) = -\pi/20$, $\dot{\phi}(0) = 0$, and the sites A and C are displaced from the drain D and source S_1 contacts, respectively. The pronounced influence of the environment on the rotational degrees of freedom is reflected in the noisy time dependence (see Fig.1b) of the speed of rotations $\Omega(t)/2\pi$, where $\Omega(t) = \dot{\phi}(t)$. Figure 1c illustrates the synchronous dynamics of loading and unloading the proton binding sites A, B, and C having populations n_A, n_B, and n_C, when they pass through the source and the drain leads. The site C is populated first because of its close proximity to the source lead S_1. The external electric field pushes the C-proton, and, correspondingly, the whole rotor unit, to turn through the angle $2\pi/3$ to the position of the minimum of the potential $U = -U_0 \cos(\phi + \phi_C)$. At this position of the rotor, the site C approaches the drain contact D and unloads the proton. At the same rotor position, the site B starts to be populated since this site is in the loading range of the source lead S_1. This leads to a subsequent 120°-turn of the rotor. The process repeats over and over, resulting in a continuous unidirectional rotation of the rotary ring. The torque, exerted by the nanomotor [6], can be defined as: $\mathcal{T} = -\sum_\sigma \left\langle n_\sigma \, \frac{dU(\phi+\phi_\sigma)}{d\phi} \right\rangle$, where $U(\phi) = -U_0 \cos\phi$ is the potential of the y-directed external electric field $\mathbf{F} = F\mathbf{y}, U_0 = Fr_0$. As follows from Fig.1d the torque oscillates between 10 and 30 pN·nm. These numbers are comparable with the torque produced by the F_0-motor of ATP synthase, but much less than the BFM torque. The torque of the motor can be increased by increasing the number of torque-generating sites.

In Fig.2 we present the dependence of the average speed of rotations, $\langle\Omega\rangle/2\pi = \langle\dot{\phi}\rangle/2\pi$ (left axis), and the average particle current, $I = -I_L = -(d/dt)\sum_k \langle c_{kL}^+ c_{kL}\rangle$ (right axis), on the difference of proton electrochemical potentials of the positive (μ_S) and the negative (μ_D) side of the membrane (proton voltage build-up, V). At the fixed voltage V the average speed of rotation is linearly proportional to the amplitude of the external electric potential U_0, up to the threshold value $U_{0,\max} = V/2$.

To demonstrate that the unidirectional rotation of the motor has an origin which is

different from the mechanisms utilizing Brownian motion of the rotary ring, we drop the fluctuation source ξ in Eq.(2) and calculate the time dependence of the angle ϕ in the absence of noise (it corresponds to the mean-field approximation for rotational degrees of freedom). To show the reversibility of rotations, in Fig.3 we switch also the direction of rotation from clockwise to counterclockwise by connecting the lead S_2 to the proton reservoir with a higher electrochemical potential (and disconnecting the lead S_1). The initial condition for the rotor angle remains the same, $\phi(0) = -\pi/20,\ \dot{\phi}(0) = 0$. This shift of the rotor position hampers the initial loading of the site B from the source S_2 (see Fig.3c), postponing the beginning of the full-scale revolutions. Nevertheless, without noise, the rotor makes more than three full rotations in 10 μs, despite the unfavorable initial conditions and despite the strong enough damping rate $\gamma = 3.6$ ns^{-1}. Note that the time dependence of the instantaneous speed of rotations $\Omega/2\pi$ (see Fig.3b) shows regular oscillations, compared with the noisy time dependence of the same variable depicted in Fig.1b. It is evident from Fig.3b that the speed of rotations oscillates synchronously with the torque generated by the motor (see Fig.3d).

Turning back to the situation with noise, we now estimate the efficiency of the nanomotor proposed above. For the parameters $U_0 = 200$ meV, and $V = 500$ meV, the average torque $\langle \mathcal{T} \rangle$ is about 20 pN·nm, while the average speed of rotations $\langle \Omega \rangle/2\pi$ is near 420 kHz (see Fig.1d and Fig.2). This means that for the output power of the motor [4] we obtain: $\langle \mathcal{T} \rangle \cdot \langle \Omega \rangle \simeq 3.3 \cdot 10^5$ eV/s. To calculate the input power provided by the proton reservoirs, we assume that the proton flux (proton current) is about $I = 1.2 \cdot 10^6$ particles per second (see Fig.2), and the voltage drop between the reservoirs is $V = 0.5$ eV. Thus, the input power can be evaluated as $I \cdot V = 6 \cdot 10^5$ eV/s. Therefore, for the efficiency of the motor, Eff $= \langle \mathcal{T} \rangle \cdot \langle \Omega \rangle / (I \cdot V)$, we obtain the estimate: Eff $\simeq 55\%$. Increasing the number of protonable sites and optimizing the system's design and parameters would improve the performance of our simple model, approaching the performance of real rotary biomotors, having an efficiency near 90%.

In summary, we have proposed a simple physical model of ion-driven rotary nanomotors which transmit the energy of an external constant electric field into mechanical motion in the presence of an electrochemical gradient. This model describes the main properties of both the F_0-motor of ATPase in mitochondria membranes and the bacterial flagellar motor *without* resorting to Brownian motion. The proposed mechanism of torque generation is based on the subsessive loading and unloading of ion-binding sites on the rotor in the presence of a dc

electric field. Our model can explain the previously mysterious phenomenon of rotational direction switching which occurs in bacterial flagellar motors. Solving jointly the Langevin-type equation and master equations for the populations of the ion-binding sites, we have determined the time evolution of the system for various values of voltages and amplitudes of the dc external electric field.

This work was supported in part by the National Security Agency, Laboratory of Physical Sciences, Army Research Office, National Science Foundation grant No. EIA-0130383, and JSPS CTC Program. S.S. acknowledges support from the EPSRC ARF No. EP/D072581/1 and AQDJJ network-programme.

---

[1] B. Alberts *et al.*, *Molecular Biology of the Cell* (Garland Science, New York, 2002), Ch. 11 and Ch. 14.

[2] W.R. Browne and B.L. Feringa, Nature Nanotechn. **1**, 25 (2006).

[3] T. Elston *et al.*, Nature **391**, 510 (1998); P. Dimroth *et al.*, Proc. Nat. Acad. Sci. USA **96**, 4924 (1999); G. Oster and H. Wang, Trends in Cell Biology **13**, 114 (2003).

[4] H.C. Berg, Annu. Rev. Biochem **72**, 19 (2003).

[5] M. Wikström, Biochem. Biophys. Acta **1655**, 241 (2004); G. Bränden *et al.*, *ibid.* **1757**, 1052 (2006); A.Yu. Smirnov *et al.*, arXiv:0711.1224 (2007).

[6] R.M. Berry, Phil. Trans. R. Soc. Lond. B **355**, 503 (2000); W.S. Ryu *et al.*, Nature **403**, 444 (2000).

[7] P. Hanggi *et al.*, Annalen der Physik **14**, 51 (2005); S. Savel'ev and F. Nori, Chaos **15**, 026112 (2005); F. Nori, Nature Physics **2**, 227 (2006).

[8] N.S. Wingreen *et al.*, Phys. Rev. B **48**, 8487 (1993); L.G. Mourokh *et al.*, Phys. Rev. B **66**, 085332 (2002).

[9] R.I. Shekhter *et al.*, J. Phys.: Condens. Matter **15**, R441 (2003); M. Blencowe, Phys. Rep. **395**, 159 (2004); A.Yu. Smirnov *et al.*, Phys. Rev. B **69**, 155310 (2004).

[10] J.K. Gimzewski *et al.*, Science **281**, 531 (1998); A.M. Fennimore *et al.*, Nature **424**, 408 (2003); G.S. Kottas *et al.*, Chem. Rev. **105**, 1281 (2005).

[11] D.J. De Rosier, Cell **93**, 17 (1998).

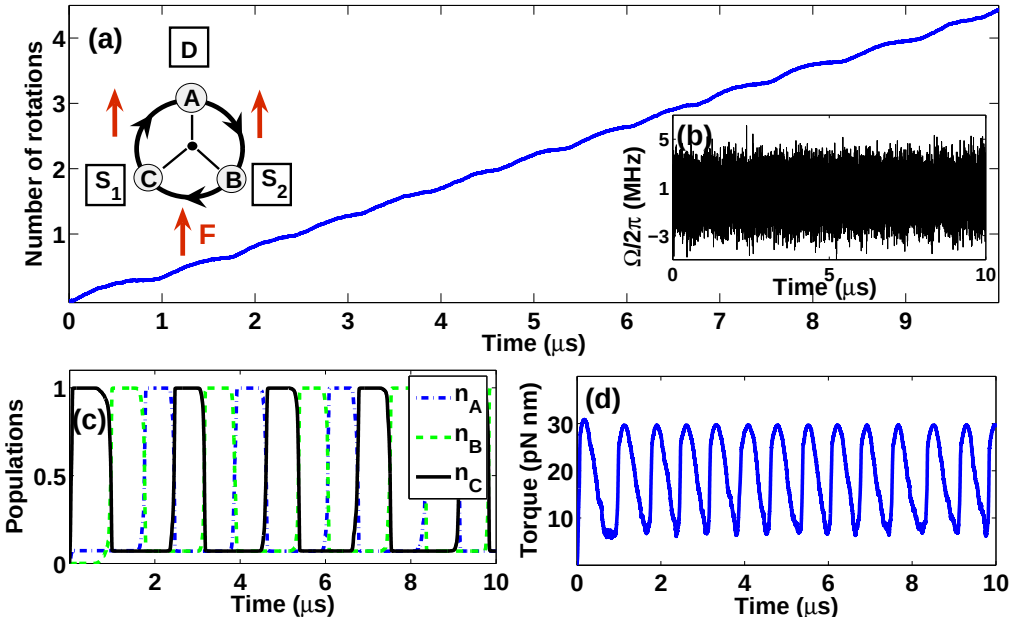

FIG. 1: (Color online) (a) Time dependence of the number of rotations $\phi(t)/2\pi$ at $V = 500$ meV, $U_0 = 200$ meV, and $T = 300$ K, with a schematic diagram of the system in the inset; (b) Stochastic dynamics of the instantaneous speed of rotation, $\Omega(t)/2\pi = \dot{\phi}(t)/2\pi$; (c) Populations of the proton-binding sites versus time; (d) Time dependence of the rotor torque in the presence of a heat bath. Notice the periodicity in (c) and (d).

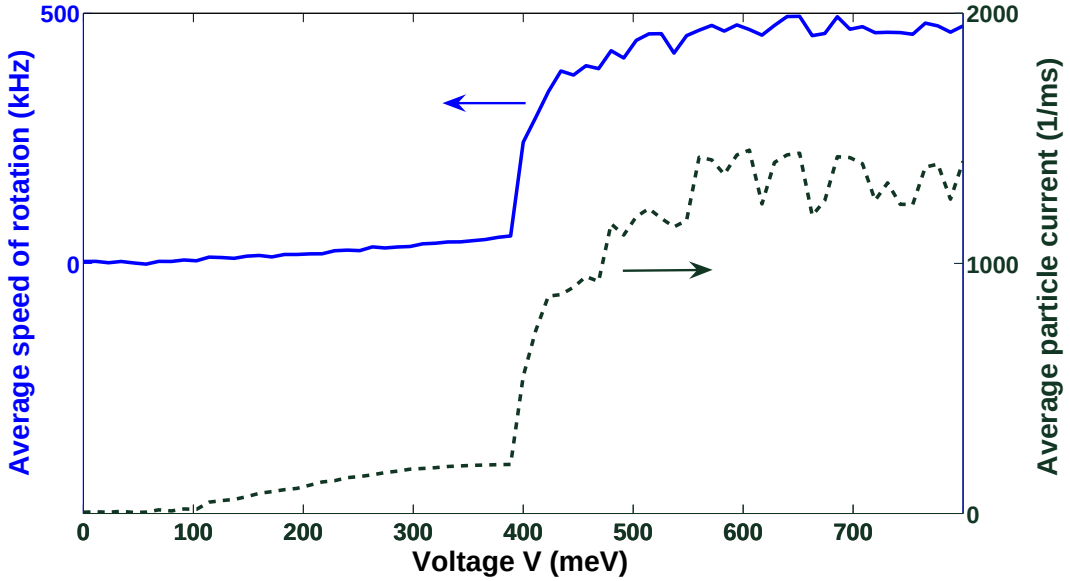

FIG. 2: (Color online) Dependence of the average speed of rotation, $\langle\Omega\rangle/2\pi$ (solid blue curve, left axis), and the average proton current, I (dashed black curve, right axis), on the proton voltage build-up, $V = \mu_S - \mu_D$, at $U_0 = 200$ meV and $T = 300$ K.

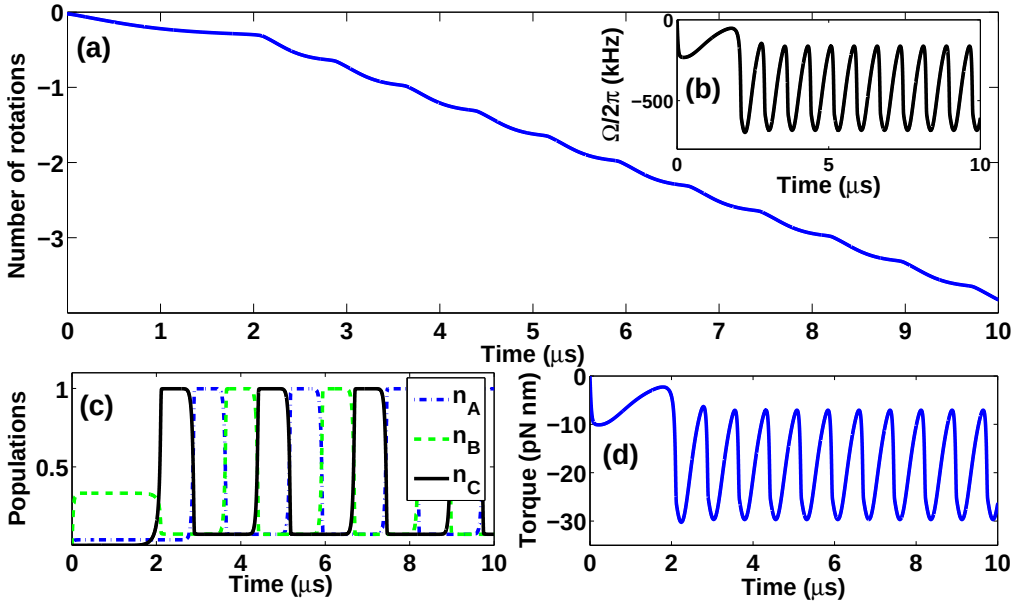

FIG. 3: (Color online) Time evolution of the system in the *absence* of external noise at $V = 500$ meV and $U_0 = 200$ meV, but now *switching* the direction of rotations: (a) number of full rotations, $\phi(t)/2\pi$, as a function of time; (b) speed of rotations, $\Omega(t)/2\pi$; (c) populations $n_A(t), n_B(t)$, and $n_C(t)$, describing the loading and unloading of the sites; (d) torque exerted by the rotor versus time.